Meccanica (2006) 41:681–691
DOI 10.1007/s11012-006-9014-x

Lie-group method of solution for steady two-dimensional boundary-layer stagnation-point flow towards a heated stretching sheet placed in a porous medium

Youssef Z. Boutros · Mina B. Abd-el-Malek · Nagwa A. Badran · Hossam S. Hassan

Received: 12 February 2005 / Accepted: 17 June 2006 / Published online: 31 October 2006

Abstract The boundary-layer equations for two-dimensional steady flow of an incompressible, viscous fluid near a stagnation point at a heated stretching sheet placed in a porous medium are considered. We apply Lie-group method for determining symmetry reductions of partial differential equations. Lie-group method starts out with a general infinitesimal group of transformations under which the given partial differential equations are invariant. The determining equations are a set of linear differential equations, the solution of which gives the transformation function or the infinitesimals of the dependent and independent variables. After the group has been determined, a solution to the given partial differential equations may be found from the invariant surface condition such that its solution leads to similarity variables that reduce the number of independent variables of the system. The effect of the velocity parameter λ, which is the ratio of the external free stream velocity to the stretching surface velocity, permeability parameter of the porous medium k_1, and Prandtl number Pr on the horizontal and transverse velocities, temperature profiles, surface heat flux and the wall shear stress, has been studied.

Keywords Boundary layer · Stagnation point flow · Porous medium · Lie-group · Mechanics of fluids

Y. Z. Boutros · M. B. Abd-el-Malek (✉) · N. A. Badran
Department of Engineering Mathematics and Physics, Faculty of Engineering, Alexandria University, Alexandria 21544, Egypt
e-mail: minab@aucegypt.edu

H. S. Hassan
Department of Basic and Applied Science, Arab Academy for Science and Technology and Maritime Transport, P.O. BOX 1029 Alexandria, Egypt.
e-mail: hossams@aast.edu

M. B. Abd-el-Malek
Present address: Department of Mathematics, The American University in Cairo, Cairo 11511, Egypt

1 Introduction

Flow and heat transfer of an incompressible viscous fluid over a stretching sheet appear in several manufacturing processes of industry such as the extrusion of polymers, the cooling of metallic plates, the aerodynamic extrusion of plastic sheets, etc. In the glass industry, blowing, floating or spinning of fibres are processes, which involve the flow due to a stretching surface [12].

Mahapatra and Gupta [7] studied the steady two-dimensional stagnation-point flow of an incompressible viscous fluid over a flat deformable sheet when the sheet is stretched in its own plane with a velocity proportional to the distance from the stagnation-point. They concluded that, for a fluid of small kinematic viscosity, a boundary layer is formed when the stretching velocity is less than the free stream velocity and an inverted boundary

layer is formed when the stretching velocity exceeds the free stream velocity. Temperature distribution in the boundary layer is determined when the surface is held at constant temperature giving the so called surface heat flux. In their analysis, they used the finite-differences scheme along with the Thomas algorithm to solve the resulting system of ordinary differential equations.

Nazar et al. [9] treated the unsteady two-dimensional boundary layer flow of a viscous and incompressible fluid in the region of the stagnation point on a stretching flat sheet, where the unsteadiness is caused by the impulsive motion of the free stream velocity and by the suddenly stretched surface. The governing equations are transformed using semi-similar coordinates originated by Williams and Rhyne [16], and Seshadri et al. [14]. The boundary layer structure of the problem is found to depend on the parameter λ, which is the ratio of the velocity of the stretching surface to that of the frictionless potential flow in the neighbourhood of the stagnation point, as deduced by Mahapatra and Gupta [7]. From an analytical investigation of the governing boundary layer equation, they have deduced solutions for the non-dimensional velocity function and the skin fraction coefficient in the initial unsteady state flow, the final steady state flow, and at small intervals.

Pop et al. [12] studied the radiation effects on the steady two-dimensional stagnation-point flow of an incompressible fluid over a stretching sheet. They have taken into account radiation effects using the Rosseland approximation to model the radiative heat transfer. This approximation leads to a considerable simplification in the radiation flux. The resulting system of ordinary differential equations is solved numerically using the Runge-Kutta method coupled with a shooting technique. The results show that, a boundary layer is formed and its thickness increases with radiation, velocity and temperature parameters and decreases when the Prandtl number is increased.

This paper is concerned with the solution of steady two-dimensional stagnation point flow of an incompressible viscous fluid over a stretching sheet which is placed in a fluid saturated porous medium. Lie-group theory is applied to the equations of motion for determining symmetry reductions of partial differential equations [1–6, 8, 10, 11, 13, 17]. The resulting system of non-linear differential equations is then solved numerically using shooting method coupled with Runge-Kutta scheme. Particular cases of our results are compared with those of Mahapatra and Gupta [7], Pop et al. [12], and Nazar et al. [9].

2 Mathematical formulation of the problem

Consider the steady, two-dimensional flow of a viscous and incompressible fluid near the stagnation point on a stretching sheet placed in the plane $\bar{y} = 0$ of a Cartesian system of coordinates $O\bar{x}\bar{y}(\bar{y} = 0)$ with the $\bar{x}$-axis along the sheet, Fig. 1. The fluid occupies the upper half plane $(\bar{y} > 0)$.The stretching surface has a uniform temperature $\bar{T}_w$ and the free stream temperature is $\bar{T}_\infty$ with $\bar{T}_w > \bar{T}_\infty$. The wall is stretched by applying two equal and opposite forces along the $\bar{x}$-axis, to keep the origin fixed.

The boundary layer equations for the steady flow of the incompressible fluid with no radiation effects, are given by

$$\frac{\partial \bar{u}}{\partial \bar{x}} + \frac{\partial \bar{v}}{\partial \bar{y}} = 0, \tag{2.1}$$

$$\bar{u}\,\frac{\partial \bar{u}}{\partial \bar{x}} + \bar{v}\,\frac{\partial \bar{u}}{\partial \bar{y}} = \bar{U}(\bar{x})\,\frac{\partial \bar{U}}{\partial \bar{x}} + \nu\,\frac{\partial^2 \bar{u}}{\partial \bar{y}^2} + \frac{\nu}{k}(\bar{U} - \bar{u}), \tag{2.2}$$

$$\bar{u}\,\frac{\partial \bar{T}}{\partial \bar{x}} + \bar{v}\,\frac{\partial \bar{T}}{\partial \bar{y}} = \alpha\,\frac{\partial^2 \bar{T}}{\partial \bar{y}^2}, \tag{2.3}$$

together with the boundary conditions

$$\begin{aligned} &\text{(i) } \bar{u} = C\bar{x}, \quad \bar{v} = 0, \quad \bar{T} = \bar{T}_w \quad \text{at } \bar{y} = 0, \\ &\text{(ii) } \bar{u} \to \bar{U}(\bar{x}) = a\bar{x}, \quad \bar{T} \to \bar{T}_\infty \quad \text{as } \bar{y} \to \infty, \end{aligned} \tag{2.4}$$

where, $\bar{u}$ is the velocity component along $\bar{x}$-axis, $\bar{v}$ is the velocity component along $\bar{y}$-axis, $\bar{U}(\bar{x})$ is the stagnation point velocity, ν is the kinematic viscosity, k is the permeability of the porous medium, $\bar{T}$ is the fluid temperature, α is the coefficient of thermal diffusivity, C and a are positive constants.

Since the surrounding medium is a fluid saturated porous medium, Eq. (2.2) is the Darcy-Forchheimer equation in which the term including the square of the velocity is neglected [15].

The variables in Eqs. (2.1)–(2.3) are dimensionless according to

$$x = \frac{C\bar{x}}{U_1}, \quad y = \sqrt{\frac{C}{\nu}}\,\bar{y}, \quad u = \frac{\bar{u}}{U_1}, \quad v = \frac{\bar{v}}{\sqrt{C\nu}},$$

$$U = \frac{\bar{U}}{U_1}, \quad T = \frac{\bar{T} - \bar{T}_\infty}{\bar{T}_w - \bar{T}_\infty}, \tag{2.5}$$

where U_1 is the characteristic velocity.

Substitution from (2.5) into (2.1)–(2.3), gives

$$\frac{\partial u}{\partial x} + \frac{\partial v}{\partial y} = 0, \tag{2.6}$$

$$u\frac{\partial u}{\partial x} + v\frac{\partial u}{\partial y} = U(x)\frac{\partial U}{\partial x} + \frac{\partial^2 u}{\partial y^2} + k_1(U-u), \tag{2.7}$$

$$u\frac{\partial T}{\partial x} + v\frac{\partial T}{\partial y} = \frac{1}{Pr}\frac{\partial^2 T}{\partial y^2}, \tag{2.8}$$

where, $k_1 = \nu/kC$ is the permeability parameter of the porous medium and $\mathrm{Pr} = \nu/\alpha$ is the Prandtl number.

The boundary conditions (2.4) will be

$$\begin{aligned} &\text{(i) } u = x, \quad v = 0, \quad T = 1 \quad \text{at } y = 0, \\ &\text{(ii) } u \to U(x) = \frac{a}{C}x, \quad T \to 0 \quad \text{as } y \to \infty. \end{aligned} \tag{2.9}$$

From the continuity Eq. (2.6), there exists a stream function $\Psi(x, y)$ such that

$$u = \frac{\partial \Psi}{\partial y}, \quad v = -\frac{\partial \Psi}{\partial x}, \tag{2.10}$$

which satisfies Eq. (2.6) identically.

Substituting from (2.10) into (2.7) and (2.8), gives

$$\begin{aligned} &\Psi_y\Psi_{xy} - \Psi_x\Psi_{yy} - UU_x - \Psi_{yyy} \\ &-k_1(U - \Psi_y) = 0, \end{aligned} \tag{2.11}$$

and

$$\Psi_y T_x - \Psi_x T_y - \frac{1}{Pr}T_{yy} = 0, \tag{2.12}$$

where subscripts denote partial derivatives.

The boundary conditions (2.9) will be

$$\begin{aligned} &\text{(i) } \Psi_y = x, \quad \Psi_x = 0, \quad T = 1 \quad \text{at } y = 0, \\ &\text{(ii) } \Psi_y \to U(x) = \frac{a}{C}x, \quad T \to 0 \quad \text{as } y \to \infty. \end{aligned} \tag{2.13}$$

3 Solution of the problem

At first, we derive the similarity solutions using the Lie-group method under which (2.11) and (2.12) are invariant.

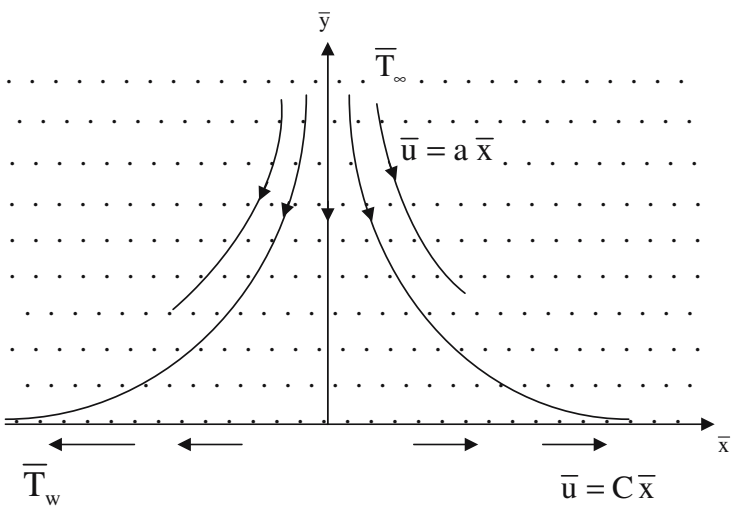

Fig. 1 Physical model and coordinate system

3.1 Lie point symmetries

Consider the one-parameter (ε) Lie group of infinitesimal transformations in (x, y, Ψ, U, T) given by

$$\begin{aligned} x^* &= x + \varepsilon\,\phi\,(x, y, \Psi, U, T) + \mathrm{O}(\varepsilon^2),\\ y^* &= y + \varepsilon\,\zeta\,(x, y, \Psi, U, T) + \mathrm{O}(\varepsilon^2),\\ \Psi^* &= \Psi + \varepsilon\,\eta\,(x, y, \Psi, U, T) + \mathrm{O}(\varepsilon^2)\\ U^* &= U + \varepsilon\,F\,(x, y, \Psi, U, T) + \mathrm{O}(\varepsilon^2),\\ T^* &= T + \varepsilon\,g\,(x, y, \Psi, U, T) + \mathrm{O}(\varepsilon^2), \end{aligned} \tag{3.1}$$

where "ε" is a small parameter.

A system of partial differential Eqs. (2.11) and (2.12) is said to admit a symmetry generated by the vector field

$$\mathrm{X} \equiv \phi\frac{\partial}{\partial x} + \zeta\,\frac{\partial}{\partial y} + \eta\frac{\partial}{\partial \Psi} + F\,\frac{\partial}{\partial U} + g\,\frac{\partial}{\partial T}, \tag{3.2}$$

if it is left invariant by the transformation $(x, y, \Psi, U, T) \to (x^*, y^*, \Psi^*, U^*, T^*)$.

The solutions $\Psi = \Psi\,(x, y)$, $U = U(x)$ and $T = T\,(x, y)$, are invariant under the symmetry (3.2) if

$$\Phi_\Psi = \mathrm{X}\,(\Psi - \Psi(x, y)) = 0 \quad \text{when} \quad \Psi = \Psi\,(x, y), \tag{3.3}$$

$$\Phi_U = \mathrm{X}\,(U - U(x)) = 0 \quad \text{when } U = U(x), \tag{3.4}$$

and

$$\Phi_T = X\,(T - T\,(x, y)) = 0 \quad \text{when } T = T\,(x, y). \tag{3.5}$$

Assume,

$$\begin{aligned} \Delta_1 &= \Psi_y\Psi_{xy} - \Psi_x\Psi_{yy} - UU_x - \Psi_{yyy}\\ &\quad -k_1(U - \Psi_y), \end{aligned} \tag{3.6}$$

$$\Delta_2 = \Psi_y T_x - \Psi_x T_y - \frac{1}{\mathrm{Pr}}T_{yy}.$$

A vector X given by (3.2), is said to be a Lie point symmetry vector field for (2.11) and (2.12) if

$$X^{[3]}\,(\Delta_j)\,\big|_{\Delta_j=0} = 0, \quad j = 1, 2, \tag{3.7}$$

where,

$$\begin{aligned} X^{[3]} \equiv\ & \phi\frac{\partial}{\partial x} + \zeta\,\frac{\partial}{\partial y} + \eta\frac{\partial}{\partial \Psi} + F\,\frac{\partial}{\partial U} + g\,\frac{\partial}{\partial T}\\ &+\eta^x\frac{\partial}{\partial \Psi_x} + \eta^y\frac{\partial}{\partial \Psi_y} + g^x\frac{\partial}{\partial T_x} + g^y\frac{\partial}{\partial T_y}\\ &+F^x\frac{\partial}{\partial U_x} + \eta^{xy}\frac{\partial}{\partial \Psi_{xy}} + \eta^{yy}\frac{\partial}{\partial \Psi_{yy}}\\ &+g^{yy}\frac{\partial}{\partial T_{yy}} + \eta^{yyy}\frac{\partial}{\partial \Psi_{yyy}}, \end{aligned} \tag{3.8}$$

is the third prolongation of X.

To calculate the prolongation of a given transformation, we need to differentiate (3.1) with respect to each of the variables, x and y. To do this, we introduce the following total derivatives:

$$\begin{aligned} D_x \equiv\ & \partial_x + \Psi_x\,\partial_\Psi + U_x\partial_U + T_x\partial_T + \Psi_{xx}\partial_{\Psi_x}\\ &+U_{xx}\partial_{U_x} + T_{xx}\partial_{T_x} + \Psi_{xy}\partial_{\Psi_y} + \cdots,\\ D_y \equiv\ & \partial_y + \Psi_y\,\partial_\Psi + T_y\partial_T + \Psi_{yy}\partial_{\Psi_y} + T_{yy}\partial_{T_y}\\ &+\Psi_{xy}\partial_{\Psi_x} + \cdots, \end{aligned} \tag{3.9}$$

Equation (3.7) gives the following system of linear partial differential equations

$$\begin{aligned} &-(U_x + k_1)\,F - \Psi_{yy}\,\eta^x + (\Psi_{xy} + k_1)\,\eta^y + \Psi_y\eta^{xy}\\ &\quad -\Psi_x\eta^{yy} - U\,F^x - \eta^{yyy} = 0,\\ &-T_y\,\eta^x + T_x\,\eta^y + \Psi_y g^x - \Psi_x\,g^y - \frac{1}{\mathrm{Pr}}g^{yy} = 0. \end{aligned} \tag{3.10}$$

The components $\eta^x, \eta^y, g^x, g^y, F^x, \eta^{xy}, \eta^{yy}, g^{yy}, \eta^{yyy}$ can be determined from the following expressions

$$\begin{aligned} \eta^S &= D_S\eta - \Psi_x\,D_S\phi - \Psi_y D_S\zeta,\\ g^N &= D_N g - T_x\,D_N\phi - T_y D_N\zeta,\\ F^x &= D_x F - U_x D_x\phi\\ \eta^{JS} &= D_S\eta^J - \Psi_{Jx}\,D_S\phi - \Psi_{Jy}D_S\zeta,\\ g^{JN} &= D_N g^J - T_{Jx}\,D_N\phi - T_{Jy}D_N\zeta, \end{aligned} \tag{3.11}$$

where S, J and N stand for x, y.

Substitution from (3.11) into (3.10) and solving the resulting equations in view of the invariance of the boundary conditions (2.13), yields

$$\begin{aligned} &\phi = C_1\,x, \quad \zeta = 0, \quad \eta = C_1\Psi + C_3, \quad F = C_1 U,\\ &g = 0. \end{aligned} \tag{3.12}$$

The system of non-linear Eqs. (2.11) and (2.12) has the two-parameter Lie group of point symmetries generated by

$$\begin{aligned} &X_1 \equiv x\frac{\partial}{\partial x} + \Psi\frac{\partial}{\partial \Psi} + U\frac{\partial}{\partial U} \quad \text{and}\\ &X_2 \equiv \frac{\partial}{\partial \Psi}. \end{aligned} \tag{3.13}$$

The one-parameter group generated by X_1 consists of scaling, whereas X_2 consists of translation. The commutator table of the symmetries is given in Table 1, where the entry in the ith row and jth column is defined as $[X_i, X_j] = X_iX_j - X_jX_i$.

Table 1 Table of commutators of the basis operators

	X_1	X_2
X_1	0	$-X_2$
X_2	X_2	0

The finite transformations corresponding to the symmetries X_1 and X_2 are respectively

$$\begin{aligned} X_1: \quad & x^* = e^{\varepsilon_1} x, \quad y^* = y, \quad \Psi^* = e^{\varepsilon_1}\Psi, \\ & U^* = e^{\varepsilon_1} U, \quad T^* = T, \\ X_2: \quad & x^* = x, \quad y^* = y, \quad \Psi^* = \Psi + \varepsilon_2, \\ & U^* = U, \quad T^* = T, \end{aligned} \tag{3.14}$$

where ε_1 and ε_2 are group parameters.
For X_2, the characteristic

$$\Phi = (\Phi_\Psi, \Phi_U, \Phi_T), \tag{3.15}$$

has the components

$$\Phi_\Psi = 1, \quad \Phi_U = 0, \quad \Phi_T = 0, \tag{3.16}$$

which means that no solutions are invariant under the group generated by X_2.
On the other hand for X_1, the characteristic (3.15) has the components

$$\begin{aligned} & \Phi_\Psi = \Psi - x\,\Psi_x, \quad \Phi_U = U - x\,U_x, \\ & \Phi_T = 0. \end{aligned} \tag{3.17}$$

Hence, the general solutions of the invariant surface conditions (3.3)–(3.5) are

$$\Psi = x\,G(y), \quad U(x) = \frac{a}{C}x, \quad T = h(y). \tag{3.18}$$

Substitution from (3.18) into (2.11) and (2.12) yields

$$\begin{aligned} & \frac{\mathrm{d}^3 G}{\mathrm{d}\,y^3} + G\frac{\mathrm{d}^2 G}{\mathrm{d}\,y^2} - \left(\frac{\mathrm{d}\,G}{\mathrm{d}\,y}\right)^2 + \lambda^2 \\ & \quad + k_1\left[\lambda - \frac{\mathrm{d}\,G}{\mathrm{d}\,y}\right] = 0, \end{aligned} \tag{3.19}$$

and

$$\frac{\mathrm{d}^2 h}{\mathrm{d}\,y^2} + \mathrm{Pr}\; G\frac{\mathrm{d}\,h}{\mathrm{d}\,y} = 0, \tag{3.20}$$

where, $\lambda = a/C$ is the velocity parameter.

The boundary conditions (2.13) will be

$$\begin{aligned} & \text{(i)} \ \frac{\mathrm{d}\,G}{\mathrm{d}\,y} = 1, \quad G = 0, \quad h = 1 \quad \text{at } y = 0, \\ & \text{(ii)} \ \frac{\mathrm{d}\,G}{\mathrm{d}\,y} \to \lambda, \quad h \to 0 \quad \text{as } y \to \infty. \end{aligned} \tag{3.21}$$

3.2 Numerical solution

The system of nonlinear differential Eqs. (3.19) and (3.20) with the boundary conditions (3.21) is solved numerically using a shooting method, coupled with Runge-Kutta scheme.
From (2.10) and (3.18), we get

$$\frac{u}{x} = \frac{\mathrm{d}\,G}{\mathrm{d}\,y}, \quad v = -G \quad \text{and} \quad T = h(y). \tag{3.22}$$

4 Results and discussion

4.1 Horizontal velocity

4.1.1 The effect of velocity parameter λ

Figure 2 illustrates the behaviour of the horizontal velocity u/x for $k_1 = 0.0$ and $k_1 = 0.1$, with Prandtl number $\mathrm{Pr} = 0.05$, over a range of velocity parameter λ. As seen, the horizontal velocity increases with the increase of λ.

A boundary layer is formed when the stretching velocity is less than the free stream velocity i.e. $\lambda > 1$. That is because, for $\lambda > 1$, the straining motion near the stagnation region increases. So, the acceleration of the external stream increases which leads to a decrease in the thickness of the boundary layer with increasing λ and as a result increasing the horizontal velocity.

Also, an inverted boundary layer is formed when the stretching velocity exceeds the free stream velocity i.e. $\lambda < 1$, in both cases when the medium is not porous, ($k_1 = 0.0$) (Fig. 2a) or when it is porous, ($k_1 = 0.1$) (Fig. 2b). For $k_1 = 0.0$, these results are in complete agreement with that reported by Mahapatra and Gupta [7] and Nazar et al. [9]. For $\lambda < 1$, the structure of the thickness boundary layer is formed bigger at $k_1 = 0.0$ than at $k_1 = 0.1$. On the other hand, for$\lambda > 1$, the structure of the thickness boundary layer is formed smaller at $k_1 = 0.0$

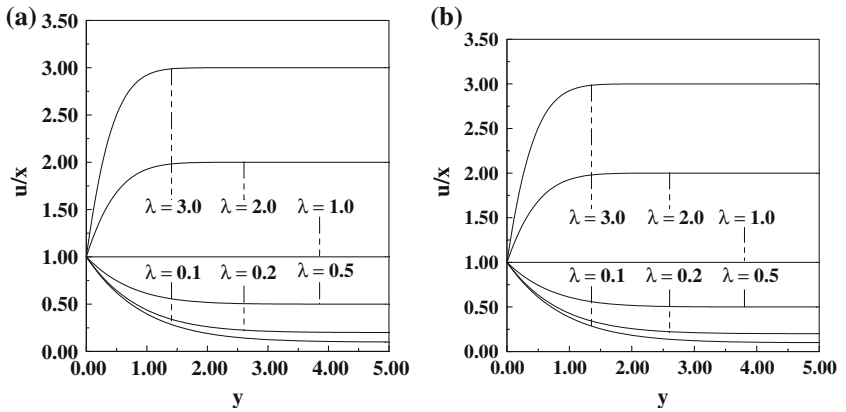

Fig. 2 Horizontal velocity profiles over a range of λ with Pr = 0.05 at: (**a**) $k_1 = 0.0$ (**b**) $k_1 = 0.1$

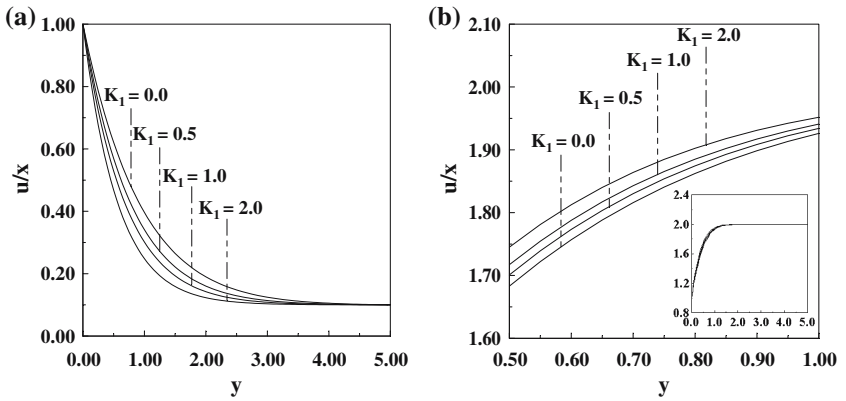

Fig. 3 Horizontal velocity profiles over a range of k_1 with Pr = 0.1 at: (**a**) λ = 0.1 (**b**) λ = 2.0

than at $k_1 = 0.1$ (Fig. 2). No boundary layer structure is formed when λ = 1.

4.1.2 The effect of the permeability parameter k_1

Figure 3 illustrates the behaviour of the horizontal velocity u/x for λ = 0.1 and λ = 2.0 with Prandtl number Pr = 0.1, over a range of the permeability parameter k_1. When λ = 0.1, the horizontal velocity decreases as k_1 increases. That is because, for λ < 1, an increase in k_1 causes an increase in boundary layer thickness and as a result a decrease in the horizontal velocity (Fig. 3a). On the other hand, when λ = 2.0, the horizontal velocity increases as k_1 increases. That is because, for λ > 1, an increase in k_1 causes a decrease in the boundary layer thickness and as a result an increase in the horizontal velocity (Fig. 3b).

4.2 Transverse velocity

4.2.1 The effect of velocity parameter λ

Figure 4 illustrates the behaviour of the transverse velocity $G(y) = -v$ for $k_1 = 0.0$ and $k_1 = 0.1$, with Prandtl number Pr = 0.05, over a range of the velocity parameter λ. It is clear that, the transverse velocity increases as λ increases.

4.2.2 The effect of the permeability parameter k_1

Figure 5 illustrates the behaviour of the transverse velocity $G(y) = -v$ for λ = 0.1 and λ = 2.0,

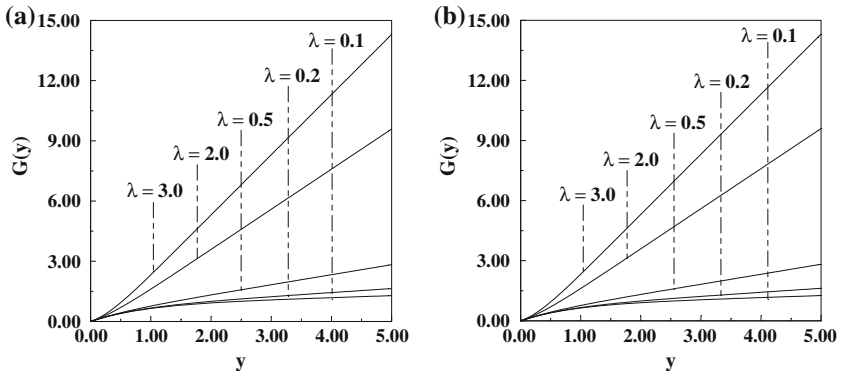

Fig. 4 Transverse velocity profiles over a range of λ with Pr = 0.05 at: (**a**) $k_1 = 0.0$ (**b**) $k_1 = 0.1$

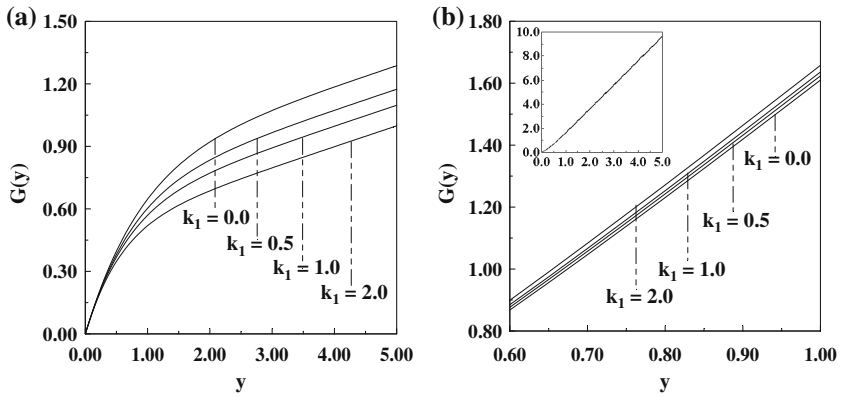

Fig. 5 Transverse velocity profiles over a range of k_1 with Pr = 0.1 at: (**a**) λ = 0.1 (**b**) λ = 2.0

with Prandtl number Pr = 0.1, over a range of the permeability parameter k_1. We note that, the transverse velocity decreases as k_1 increases when λ < 1 (Fig. 5a), while a slight variation in the rate of increase of the transverse velocity appears with increasing k_1 when λ > 1 (Fig. 5b).

4.3 The temperature profiles

4.3.1 The effect of velocity parameter λ

Figure 6 illustrates the variation of the temperature profiles T for $k_1 = 0.0$ and $k_1 = 0.1$, with Prandtl number Pr = 0.05, over a range of the velocity parameter λ. We notice that, the temperature profiles decrease as λ increases and therefore the thinning of the thermal boundary layer. In case of $k_1 = 0.0$, our result is in complete agreement with that reported by Mahapatra and Gupta [7] and Pop et al. [12]. A small variation in the rate of decrease of T appears when λ > 1 and this variation becomes more evident when λ < 1 (Fig. 6).

4.3.2 The effect of the permeability parameter k_1

Figure 7 illustrates the variation of the temperature profiles T for λ = 0.1(< 1.0) with Prandtl number Pr = 0.05 and Pr = 0.1, over a range of the permeability parameter k_1. The temperature increases as k_1 increases. A small variation in the rate of increase of T appears when Pr = 0.1 (Fig. 7b), and this variation becomes slightly evident when Pr = 0.05 (Fig. 7a).

Figure 8 illustrates the variation of the temperature profiles T for λ = 2.0(> 1.0) with Prandtl

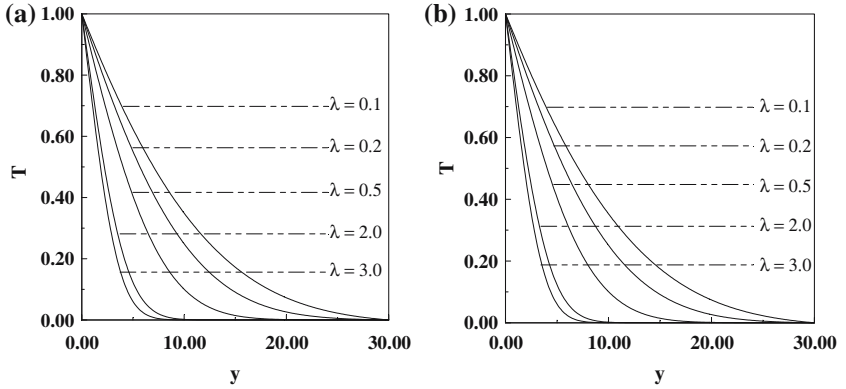

Fig. 6 Temperature profiles over a range of λ with Pr $= 0.05$ at: (**a**) $k_1 = 0.0$ (**b**) $k_1 = 0.1$

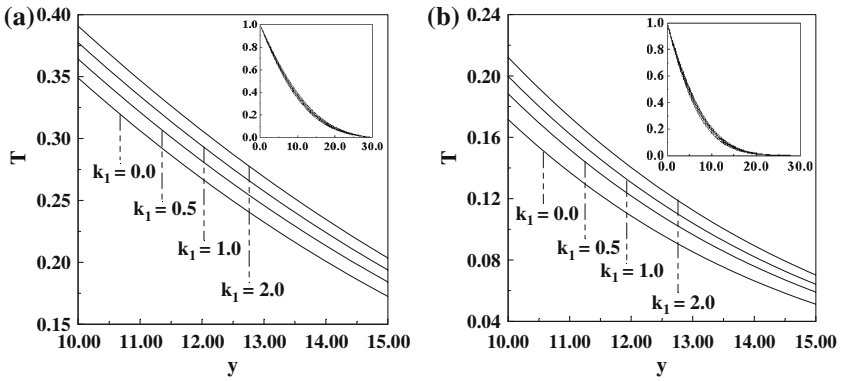

Fig. 7 Temperature profiles over a range of k_1 with $\lambda = 0.1$ at: (**a**) Pr $= 0.05$ (**b**) Pr $= 0.1$

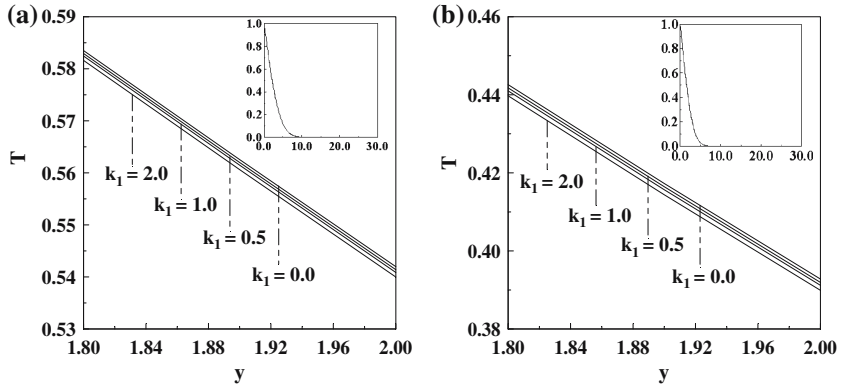

Fig. 8 Temperature profiles over a range of k_1 with $\lambda = 2.0$ at: (**a**) Pr $= 0.05$ (**b**) Pr $= 0.1$

number Pr $= 0.05$ and Pr $= 0.1$, over a range of the permeability parameter k_1. Here, a slight variation in the rate of decrease of the temperature T appears in both cases, as k_1 increases.

4.3.3 The effect of the Prandtl number Pr

Figure 9 illustrates the variation of the temperature profiles T for $\lambda = 0.1$ and $k_1 = 0.1$, over a

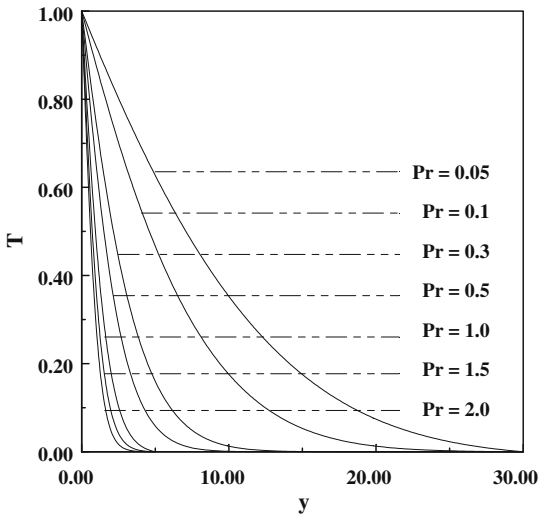

Fig. 9 Temperature profiles over a range of Pr at $\lambda = 0.1$ and $k_1 = 0.1$

range of Prandtl number Pr. It is noticed that, as Pr decreases, the thickness of the thermal boundary layer becomes greater than the thickness of the velocity boundary layer according to the well-known relation $\frac{\delta_T}{\delta} \approx (\mathrm{Pr})^{-1/2}$, where δ_T is the thickness of the thermal boundary layer and δ is the thickness of the velocity boundary layer. So, the thickness of the thermal boundary layer increases as Pr decreases and hence, the temperature T decreases with the increase of Pr (Fig. 9)

4.4 Surface heat flux

As mentioned before, when the Prandtl number increases, the thickness of thermal boundary layer becomes thinner and this causes an increase in the gradient of the temperature. Therefore, the surface heat flux $(-h'(0))$ increases as Pr increases. For different values of the velocity parameter λ and Prandtl number Pr at $k_1 = 0.0$, computed values of the surface heat flux are compared with those obtained by Mahapatra and Gupta [7] and Pop et al. [12]. The results are in very good agreement, Table 2.

From Table 2, it is noticed that, for fixed value of Pr, the surface heat flux $(-h'(0))$ increases as the velocity parameter λ increases. Also, the value of $(-h'(0))$ is positive which is consistent with the fact that the heat flows from the surface to the fluid as long as $\bar{T}_w > \bar{T}_\infty$ in the absence of viscous dissipation.

4.5 Wall shear stress

The dimensionless wall shear stress $G''(0)$ (skin friction) is computed for different values of the velocity parameter λ and permeability parameter k_1 at $\mathrm{Pr} = 0.05$. As seen from Table 3, the absolute value of the dimensionless wall shear stress $\left| G''(0) \right|$ decreases as λ increases when $\lambda < 1$ and it increases with increasing λ when $\lambda > 1$which is consistent with the fact that, there is progressive thinning of the boundary layer with increasing λ. Also, the absolute value of the dimensionless wall shear stress $\left| G''(0) \right|$ increases as $k_1$increases for fixed value of velocity parameter λ (Table 3).

The computed values of $G''(0)$ are compared with those obtained by Mahapatra and Gupta [7], Pop et al. [12], and Nazer et al. [9], for different values of the velocity parameter $\lambda$and with Prandtl number $\mathrm{Pr} = 0.05$ at $k_1 = 0.0$. The results are in complete agreement (Table 4).

Table 2 Comparison between the values of $h'(0)$ at $k_1 = 0.0$ for different values of λ and Pr

λ	Mahapatra and Gupta (2002) Pr			Pop et al. (2004) Pr			Present work Pr		
	0.5	1.0	1.5	0.5	1.0	1.5	0.5	1.0	1.5
0.1	−0.383	−0.603	−0.777	−0.381	−0.600	−0.773	−0.3827	−0.6048	−0.7770
0.2	−0.408	−0.625	−0.797	−0.406	−0.621	−0.793	−0.4073	−0.6256	−0.7972
0.5	−0.473	−0.692	−0.863	−0.471	−0.689	−0.859	−0.4728	−0.6925	−0.8648
1.0	−0.563	−0.796	−0.974	−0.562	−0.793	−0.970	−0.5641	−0.7979	−0.9772
2.0	−0.709	−0.974	−1.171	−0.708	−0.971	−1.168	−0.7118	−0.9787	−1.1781
3.0	−0.829	−1.124	−1.341	−0.828	−1.122	−1.339	−0.8335	−1.1321	−1.1352

Table 3 Values of dimensionless wall shear stress $G''(0)$ for different λ and k_1

λ	$G''(0)$ k_1					
	0.0	0.1	0.5	1.0	1.5	2.0
0.1	− 0.969643	− 1.010073	− 1.158373	− 1.321118	− 1.466126	− 1.598121
0.2	− 0.918164	− 0.951899	− 1.076833	− 1.215624	− 1.340381	− 1.454602
0.5	− 0.667259	− 0.685439	− 0.754013	− 0.832126	− 0.903694	− 0.970102
2.0	2.017506	2.041796	2.136322	2.249105	2.356671	2.459670
3.0	4.729285	4.770855	4.933765	5.130383	5.319968	5.503211

Table 4 Comparison between the values of $G''(0)$ at $k_1 = 0.0$ and $\Pr = 0.05$ for different values of λ

λ	$G''(0)$			
	Mahapatra and Gupta (2002)	Pop et al. (2004)	Nazar et al.(2004)	Present work
0.1	− 0.9694	− 0.9694	− 0.9694	− 0.969643
0.2	− 0.9181	− 0.9181	− 0.9181	− 0.918164
0.5	− 0.6673	− 0.6673	− 0.6673	− 0.667259
2.0	2.0175	2.0174	2.0176	2.017506
3.0	4.7293	4.7290	4.7296	4.729285

5 Conclusion

Lie-group method is applicable to both linear and non-linear partial differential equations, which leads to similarity variables that may be used to reduce the number of independent variables in partial differential equations. By determining the transformation group under which a given partial differential equation is invariant, we can obtain information about the invariants and symmetries of that equation. This information can be used to determine the similarity variables that will reduce the number of independent variables in the system. In this work, we have used Lie symmetry techniques to obtain similarity reductions of nonlinear boundary layer Eqs. (2.1)–(2.3), for the two-dimensional steady flow of an incompressible, viscous fluid near a stagnation point at a heated stretching sheet placed in a porous medium. By determining the transformation group under which a given partial differential equation is invariant, we obtained information about the invariants and symmetries of that equation. This information, in turn, was used to determine the similarity variables that reduced the number of independent variables.

The resulting system of non-linear ordinary differential Eqs. (3.19)–(3.20) is solved numerically with the boundary conditions (3.21) using shooting method, coupled with Runge-Kutta scheme. We have studied the effects of the velocity parameter λ, the permeability parameter k_1 and the Prandtl number Pr on the horizontal velocity u/x, transverse velocity $G(y) = -v$, temperature profiles T, surface heat flux $(-h'(0))$ and the wall shear stress. Particular cases of our results are compared with those of Mahapatra and Gupta [7], Pop et al. [12], and Nazar et al. [9] and were found to agree very well with their results.

Acknowledgements The authors would like to express their sincere thank the reviewers for suggesting certain changes in the original manuscript, for their valuable comments which improved the paper and for their great interest in that work.

References

1. Basarab P, Lahno V (2002) Group classification of nonlinear partial differential equations: a new approach to resolving the problem. Proc Institute of Mathematics of NAS of Ukraine 43:86–92
2. Burde GI (2002) Expanded Lie group transformations and similarity reductions of differential equations. Proc Institute of Mathematics of NAS of Ukraine 43:93–101
3. Gandarias ML, Bruzon MS (1998) Classical and nonclassical symmetries of a generalized Boussinesq equation. J Nonlinear Mathematical Phys 5:8–12

4. Hill JM (1982) Solution of differential equations by means of one-parameter groups. Pitman Publishing Co., Marshfield, MA
5. Hydon PE (2000) Symmetry methods for differential equations. CUP, Cambridge
6. Ibragimov NH (1999) Elementary Lie group analysis and ordinary differential equations. Wiley, New York
7. Mahapatra TR, Gupta AS (2002) Heat transfer in stagnation – point flow towards a stretching sheet. J Heat Mass Transfer 38:517–521
8. Moritz B, Schwalm W, Uherka D (1998) Finding Lie groups that reduce the order of discrete dynamical systems. J Phys A: Math 31:7379–7402
9. Nazar R, Amin N, Filip D, Pop I (2004) Unsteady boundary layer flow in the region of the stagnation point on a stretching sheet. Int J Eng Sci 42:1241–1253
10. Nucci MC, Clarkson PA (1992) The nonclassical method is more general than the direct method for symmetry reductions. An example of the Fitzhugh-Nagumo equation. Phys Lett A 164:49–56
11. Olver PJ (1986) Applications of Lie Groups to differential equations. New-York, Springer-Verlag
12. Pop SR, Grosan T, Pop I (2004) Radiation effects on the flow near the stagnation point of a stretching sheet. TECHNISCHE MECHANIK, Band 25, Heft 2:100–106
13. Seshadri R, Na TY (1985) Group invariance in engineering boundary value problems. Springer-Verlag, New York
14. Seshadri R, Sreeshylan N, Nath G (2002) Unsteady mixed convection flow in the stagnation region of a heated vertical plate due to impulsive motion. Int J Heat Mass Transfer 45:1345–1352
15. Vafai K, Tien CL (1981) Boundary and inertia effects on flow and heat transfer in porous media. Int J Heat Mass Transfer 24:195–203
16. Williams JC, Rhyne TH (1980) Boundary layer development on a wedge impulsively set into motion. SIAM J App Math 38:215–224
17. Yi Z, Fengxiang M (2000) Lie symmetries of mechanical systems with unilateral holonomic constraints. Chinese Sci Bull 45:1354–1358